Atmospheric
Chemistry
and Physics
Discussions

1    Formation mechanisms of atmospheric nitrate and sulfate during the

2    winter haze pollution periods in Beijing: gas-phase, heterogeneous

3    and aqueous-phase chemistry

4    **Pengfei Liu**[1, 2, 3, 5]**, Can Ye**[1, 3]**, Chaoyang Xue**[1, 3]**, Chenglong Zhang**[1, 2, 3]**, Yujing Mu**[1, 2, 3, 4]**, Xu**

5    **Sun**[1, 6]

6    [1] Research Center for Eco-Environmental Sciences, Chinese Academy of Sciences, Beijing, 100085, China.

7    [2] Center for Excellence in Urban Atmospheric Environment, Institute of Urban Environment, Chinese Academy of

8    Sciences, Xiamen, 361021, China.

9    [3] University of Chinese Academy of Sciences, Beijing, 100049, China.

10    [4] National Engineering Laboratory for VOCs Pollution Control Material & Technology, University of Chinese

11    Academy of Sciences, Beijing, 100049, China.

12    [5] Key Laboratory of Atmospheric Chemistry, China Meteorological Administration, Beijing, 100081, China.

13    [6] Beijing Urban Ecosystem Research Station, Beijing, 100085, China.

14    **Correspondence: Yujing Mu** (yjmu@rcees.ac.cn)

15    **Abstract**

16    A vast area in China is currently going through severe haze episodes with drastically elevated

17    concentrations of $PM_{2.5}$ in winter. Nitrate and sulfate are main constituents of $PM_{2.5}$ but their

18    formations via $NO_2$ and $SO_2$ oxidation are still not comprehensively understood, especially under

19    different pollution or atmospheric relative humidity (RH) conditions. To elucidate formation

20    pathways of nitrate and sulfate in different polluted cases, hourly samples of $PM_{2.5}$ were collected

21    continuously in Beijing during the wintertime of 2016. Three serious pollution cases were

22    identified reasonably during the sampling period and the secondary formations of nitrate and

23    sulfate were found to make a dominant contribution to atmospheric $PM_{2.5}$ under the relatively high

24    RH condition. The significant correlation between NOR and $NO_2 \times O_3$ during the nighttime under

25    the RH≥60% condition indicated that the heterogeneous hydrolysis of $N_2O_5$ involving aerosol

26    liquid water was responsible for the nocturnal formation of nitrate at the extremely high RH levels.

27    The more coincident trend of NOR and HONO × DR (direct radiation) × $NO_2$ than Dust × $NO_2$

28  during the daytime under the 30%<RH<60% condition provided convincing evidence that the

29  gas-phase reaction of $NO_2$ with OH played a pivotal role in the diurnal formation of nitrate at

30  moderate RH levels. The extremely high mean values of SOR during the whole day under the

31  RH≥60% condition could be ascribed to the evident contribution of $SO_2$ aqueous-phase oxidation

32  to the formation of sulfate during the severe pollution episodes. Based on the parameters measured

33  in this study and the known sulfate production rate calculation method, the oxidation pathway of

34  $H_2O_2$ rather than $NO_2$ was found to contribute greatly to the aqueous-phase formation of sulfate.

35  **1. Introduction**

36      In recent years, severe haze has occurred frequently in Beijing as well as the North China

37  Plain (NCP) during the wintertime, which has aroused great attention from the public due to its

38  adverse impact on atmospheric visibility, air quality and human health (Chan and Yao,

39  2008;Zhang et al., 2012;Zhang et al., 2015).

40      To mitigate the severe haze pollution situations, a series of regulatory measures for primary

41  pollution sources have been implemented by the Chinese government. For example, coal

42  combustion for heating in winter has gradually been replaced with electricity and natural gas in

43  the NCP, coal-fired power plants have been strictly required to install flue-gas denitration and

44  desulfurization systems (Chen et al., 2014), the stricter control measures such as terminating

45  production in industries and construction as well as the odd and even number rule for vehicles

46  have been performed in megacities during the period of the red alert for haze and so on. These

47  actions have made tremendous effects to decline pollution levels of primary pollutants including

48  $PM_{2.5}$ (fine particulate matter with an aerodynamic diameter less than 2.5 μm) in recent years (Li

49  et al., 2019). However, the serious pollution events still occurred in many areas of

50    Beijing-Tianjin-Hebei (BTH) region in December 2016 and January 2017 (Li et al., 2019). It has

51    been acknowledged that the severe haze pollution is mainly ascribed to stagnant meteorological

52    conditions with high atmospheric relative humidity (RH) and low mixed boundary layer height,

53    strong emissions of primary gaseous pollutants and rapid formation of secondary inorganic

54    aerosols (SIAs, the sum of sulfate, nitrate and ammonium), especially sulfate and nitrate (Cheng et

55    al., 2016;Guo et al., 2014;Huang et al., 2014). Some studies suggested that the contribution of

56    SIAs to $PM_{2.5}$ was higher than 50 % during the most serious haze days (Quan et al., 2014;Xu et al.,

57    2017;Zheng et al., 2015a).

58        Generally, atmospheric sulfate and nitrate are formed through the oxidations of the precursor

59    gases ($SO_2$ and $NO_2$) by oxidants (e.g. OH radical, $O_3$) via gas-phase, heterogeneous and

60    aqueous-phase reactions (Ravishankara, 1997;Wang et al., 2013;Yang et al., 2015). It should be

61    noted that the recent study proposed the remarkable emissions of primary sulfate from residential

62    coal combustion with the sulfur contents of coal in range of 0.81-1.88 % in Xi'an (Dai et al.,

63    2019), but the primary emissions of sulfate could be neglected due to the extremely low sulfur

64    content of coal (0.26-0.34 %) used prevailingly in the NCP (Du et al., 2016;Li et al., 2016).

65    Atmospheric RH is a key factor that facilitates the SIAs formation and aggravates the haze

66    pollution (Wu et al., 2019), and hence the secondary formations of sulfate and nitrate are simply

67    considered to be mainly via gas-phase reaction at relatively low atmospheric RH levels (RH<30 %)

68    and heterogeneous reactions and aqueous-phase reactions at relatively high atmospheric RH levels

69    (RH>60 %) (Li et al., 2017). However, their formation mechanisms at different atmospheric RH

70    levels still remain controversial and unclear (Cheng et al., 2016;Ge et al., 2017;Guo et al., 2017;Li

71    et al., 2018;Liu et al., 2017a;Wang et al., 2016;Yang et al., 2017). For example, the recent studies

72    proposed that atmospheric $SO_2$ oxidation by $NO_2$ dissolved in aqueous aerosol phases under the

73    extremely high atmospheric RH conditions played a dominant role in sulfate formation under

74    almost neutral aerosol solutions (a pH range of 5.4-7.0) during the serious pollution periods

75    (Cheng et al., 2016;Wang et al., 2018a;Wang et al., 2016). However, Liu et al. (2017a) and Guo et

76    al. (2017) found that the aerosol pH estimated by ISORROPIA-II model was moderately acidic (a

77    pH range of 3.0-4.9) and thus the pathway of $SO_2$ aqueous-phase oxidation by dissolved $NO_2$ was

78    unimportant during severe haze events in China. Additionally, although the pathway of $N_2O_5$

79    heterogeneous hydrolysis has been recognized as being responsible for the nocturnal formation of

80    $NO_3^-$ under relatively high atmospheric RH conditions (Tham et al., 2018;Wang et al.,

81    2018b;Wang et al., 2018c), the effects of $NO_2$ gas-phase chemistry and $NO_2$ heterogeneous

82    chemistry on the diurnal formation of $NO_3^-$ under moderate atmospheric RH conditions

83    (30 %<RH<60 %) have not yet been understood. Therefore, measurements of the species in $PM_{2.5}$

84    in different polluted cases during the wintertime are urgently needed to elucidate formation

85    pathways of sulfate and nitrate.

86       In this study, hourly filter samples of $PM_{2.5}$ were collected continuously in Beijing during the

87    wintertime of 2016, and the pollution characteristics and formation mechanisms of sulfate and

88    nitrate in the $PM_{2.5}$ samples were investigated comprehensively under different atmospheric RH

89    conditions in relation to gas-phase, heterogeneous and aqueous-phase chemistry.

90    **2. Materials and Methods**

91    **2.1. Sampling and analysis**

92       The sampling site was chosen on the rooftop (around 25 m above the ground) of a six-story

93    building in Research Center for Eco-Environmental Sciences, Chinese Academy of Sciences

Atmospheric
Chemistry
and Physics
Discussions

Open Access

EGU

94    (RCEES, CAS), which was located in the northwest of Beijing and had been described in detail by

95    our previous studies (Liu et al., 2016a;Liu et al., 2017b). The location of the sampling site

96    (40°00′29.85″ N, 116°20′29.71″ E) is presented in Figure S1. Hourly $PM_{2.5}$ samples were collected

97    on prebaked quartz fiber filters (90mm, Munktell) from January 7th to 23th of 2016 by

98    median-volume samplers (Laoying-2030) with a flow rate of 100 L min$^{-1}$. Water-soluble ions

99    (WSI), including $Na^+$, $NH_4^+$, $Mg^{2+}$, $Ca^{2+}$, $K^+$, $Cl^-$, $NO_2^-$, $NO_3^-$ and $SO_4^{2-}$, as well as carbon

100   components including organic carbon (OC) and element carbon (EC) in the filter samples were

101   analyzed by ion chromatography (Wayeal IC6200) and thermal optical carbon analyzer

102   (DRI-2001A), respectively (Liu et al., 2017b). Analysis relevant for quality assurance & quality

103   control (QA/QC) was presented in detail in section M1 of the Supplementary Information (SIs).

104   Atmospheric $H_2O_2$ and HONO were monitored by AL2021-$H_2O_2$ monitor (AERO laser, Germany)

105   and a set of double-wall glass stripping coil sampler coupled with ion chromatography (SC-IC),

106   respectively (Ye et al., 2018;Xue et al., 2019a;Xue et al., 2019b). More details about the

107   measurements of $H_2O_2$ and HONO were ascribed in section M2 of the SIs. Meteorological data,

108   including wind speed, wind direction, ambient temperature and RH, as well as air quality index

109   (AQI) derived by $PM_{2.5}$, $SO_2$, $NO_x$, CO and $O_3$ were obtained from Beijing urban ecosystem

110   research station in RCEES, CAS (http://www.bjurban.rcees.cas.cn/).

111   **2.2. Aerosol liquid water contents and pH prediction by ISORROPIA-II model**

112        The ISORROPIA-II model was employed to calculate the equilibrium composition for

113   $Na^+$-$K^+$-$Ca^{2+}$-$Mg^{2+}$-$NH_4^+$-$Cl^-$-$NO_3^-$-$SO_4^{2-}$-$H_2O$ aerosol system, which is widely used in regional

114   and global atmospheric models and has been successfully applied in numerous studies for

115   predicting the physical state and composition of atmospheric inorganic aerosols (Fountoukis and

116    Nenes, 2007;Guo et al., 2015;Shi et al., 2017). It can be used in two modes: forward mode and

117    reverse mode. Forward mode calculates the equilibrium partitioning given the total concentrations

118    of gas and aerosol species, whereas reverse mode involves predicting the thermodynamic

119    compositions based only on the concentrations of aerosol components. Forward mode was

120    adopted in this study because reverse mode calculations have been verified to be not suitable to

121    characterize aerosol acidity (Guo et al., 2015;Hennigan et al., 2015;Murphy et al., 2017;Pathak et

122    al., 2004;Weber et al., 2016). The ISORROPIA-II model is available in "metastable" or "solid +

123    liquid" state solutions. Considering the relatively high RH during the sampling period, the

124    metastable state solution was selected in this study due to its better performance than the latter

125    (Bougiatioti et al., 2016;Guo et al., 2015;Liu et al., 2017a;Weber et al., 2016). Additionally,

126    although the gaseous $HNO_3$, $H_2SO_4$, HCl and $NH_3$ were not measured in this study, gas-phase

127    input with the exception of $NH_3$ has an insignificant impact on the aerosol liquid water contents

128    (ALWC) and pH calculation due to the lower concentrations of $HNO_3$, $H_2SO_4$ and HCl than $NH_3$

129    in the atmosphere (Ding et al., 2019;Guo et al., 2017). Based on the long-term measurement in the

130    winter of Beijing, an empirical equation between $NO_x$ and $NH_3$ concentrations was derived from

131    the previous study (Meng et al., 2011), that is, $NH_3$ (ppb) = 0.34 × $NO_x$ (ppb) + 0.63, which was

132    employed for estimating the $NH_3$ concentration in this study. The predicted daily average

133    concentrations of $NH_3$ varied from 3.3 µg m$^{-3}$ to 36.9 µg m$^{-3}$, with a mean value of 16.6 µg m$^{-3}$

134    and a median value of 14.6 µg m$^{-3}$, which were in line with those (7.6-38.1 µg m$^{-3}$, 18.2 µg m$^{-3}$

135    and 16.2 µg m$^{-3}$ for the daily average concentrations, the mean value and the median value of $NH_3$,

136    respectively) during the winter of 2013 in Beijing in the previous study (Zhao et al., 2016).

137        Then, the aerosol pH could be calculated by the following equation:

138 $$pH = -log_{10}\frac{1000 \times H^+}{W}$$

139 where $H^+$ (μg m$^{-3}$) and $W$ (μg m$^{-3}$) are the equilibrium particle hydrogen ion concentration

140 and aerosol water contents, respectively, both of which could be output from ISORROPIA-II.

141 **2.3. Production of sulfate in aqueous-phase reactions**

142 The previous studies showed that there were six pathways of the aqueous-phase oxidation of

143 $SO_2$ to the production of sulfate, i.e. $H_2O_2$ oxidation, $O_3$ oxidation, $NO_2$ oxidation, transition metal

144 ions (TMI) + $O_2$ oxidation, methyl hydrogen peroxide (MHP) oxidation and peroxyacetic acid

145 (PAA) oxidation (Cheng et al., 2016;Zheng et al., 2015a). Because some TMIs, such as Ti(III),

146 V(III), Cr(III), Co(II), Ni(II), Cu(II) and Zn(II), displayed much less catalytic activities (Cheng et

147 al., 2016), only Fe(III) and Mn(II) were considered in this study. In addition, due to the extremely

148 low concentrations of MHP and PAA in the atmosphere, their contributions to the production of

149 sulfate could be ignored (Zheng et al., 2015a). To investigate the formation mechanism of sulfate

150 during the serious pollution episodes, the contributions of $O_3$, $H_2O_2$, $NO_2$ and Fe(III) + Mn(II) to

151 the production of sulfate in aqueous-phase reactions were calculated by the formulas as follows

152 (Cheng et al., 2016;Ibusuki and Takeuchi, 1987;Seinfeld and Pandis, 2006):

153 $$-(\frac{d[S(IV)]}{dt})_{O_3} = (k_0[SO_2 \cdot H_2O] + k_1[HSO_3^-] + k_2[SO_3^{2-}])[O_{3(aq)}] \qquad \text{(R1)}$$

154 $$-(\frac{d[S(IV)]}{dt})_{H_2O_2} = \frac{k_3[H^+][HSO_3^-][H_2O_{2(aq)}]}{1+K[H^+]} \qquad \text{(R2)}$$

155 $$-(\frac{d[S(IV)]}{dt})_{Fe(III)+Mn(II)} = k_4[H^+]^a[Mn(II)][Fe(III)][S(IV)] \qquad \text{(R3)}$$

156 $$-(\frac{d[S(IV)]}{dt})_{NO_2} = k_5[NO_{2(aq)}][S(IV)] \qquad \text{(R4)}$$

157 where $k_0 = 2.4 \times 10^4$ M$^{-1}$ s$^{-1}$, $k_1 = 3.7 \times 10^5$ M$^{-1}$ s$^{-1}$, $k_2 = 1.5 \times 10^9$ M$^{-1}$ s$^{-1}$, $k_3 = 7.45 \times 10^7$ M$^{-1}$ s$^{-1}$, K =

158 13 M$^{-1}$, $k_4 = 3.72 \times 10^7$ M$^{-1}$ s$^{-1}$, a = -0.74 (pH≤4.2) or $k_4 = 2.51 \times 10^{13}$ M$^{-1}$ s$^{-1}$, a = 0.67 (pH>4.2), and

159 $k_5 = (1.24-1.67) \times 10^7$ M$^{-1}$ s$^{-1}$ (5.3≤pH≤8.7, the linear interpolated values were used for pH between

160   5.3 and 8.7) at 298 K (Clifton et al., 1988); $[O_{3(aq)}]$, $[H_2O_{2(aq)}]$ and $[NO_{2(aq)}]$ could be calculated by

161   the Henry's constants which are $1.1 \times 10^{-2}$ M atm$^{-1}$, $1.0 \times 10^5$ M atm$^{-1}$ and $1.0 \times 10^{-2}$ M atm$^{-1}$ at 298 K

162   for $O_3$, $H_2O_2$ and $NO_2$ respectively (Seinfeld and Pandis, 2006). As for [Fe(III)] and [Mn(II)], their

163   concentrations entirely depended on the values of pH due to the precipitation equilibriums of

164   Fe(OH)$_3$ and Mn(OH)$_2$ (Graedel and Weschler, 1981). Considering the aqueous-phase ionization

165   equilibrium of $SO_2$, the Henry's constants of HSO$_3^-$, SO$_3^{2-}$ and S(IV) could be expressed by the

166   equations as follows (Seinfeld and Pandis, 2006):

$$H^*_{HSO_3^-} = H_{SO_2} \frac{K_{S1}}{[H^+]} \qquad (R5)$$

$$H^*_{SO_3^{2-}} = H_{SO_2} \frac{K_{S1}K_{S2}}{[H^+]^2} \qquad (R6)$$

$$H^*_{S(IV)} = H_{SO_2} \left(1 + \frac{K_{S1}}{[H^+]} + \frac{K_{S1}K_{S2}}{[H^+]^2}\right) \qquad (R7)$$

170   where $H_{SO2} = 1.23$ M atm$^{-1}$, $K_{S1} = 1.3 \times 10^{-2}$ M and $K_{S2} = 6.6 \times 10^{-8}$ M at 298 K. In addition, all

171   of rate constants (k), Henry's constants (H) and ionization constants (K) are evidently influenced

172   on the ambient temperature and are calibrated by the formulas as follows (Seinfeld and Pandis,

173   2006):

$$k(T) = k(T_0)e^{\left[-\frac{E}{R}\left(\frac{1}{T}-\frac{1}{T_0}\right)\right]} \qquad (R8)$$

$$H(T) = H(T_0)e^{\left[-\frac{\Delta H}{R}\left(\frac{1}{T}-\frac{1}{T_0}\right)\right]} \qquad (R9)$$

$$K(T) = K(T_0)e^{\left[-\frac{E}{R}\left(\frac{1}{T}-\frac{1}{T_0}\right)\right]} \qquad (R10)$$

177   where T is the ambient temperature, $T_0$=298 K, both E/R and ΔH/R varied in the different

178   equations and their values could be found in Cheng et al., (2016).

179   Furthermore, mass transport was also considered for multiphase reactions in different

180   medium and across the interface in section M3 of the SIs.

181   **3. Results and Discussion**

### 3.1. Variation characteristics of the species in $PM_{2.5}$ and typical gaseous pollutants

182

183     The concentrations of the species in $PM_{2.5}$ and typical gaseous pollutants including $NO_x$, $SO_2$,

184     $O_3$, HONO and $H_2O_2$ as well as atmospheric RH are shown in Figure 1. The meteorological

185     parameters (wind speed, wind direction, ambient temperature and direct radiation (DR)) as well as

186     the concentrations of $PM_{2.5}$ are displayed in Figure S2. During the sampling period, the

187     concentrations of the species in $PM_{2.5}$ and typical gaseous pollutants varied similarly on a

188     timescale of hours with a distinct periodic cycle of 3-4 days, suggesting that meteorological

189     conditions played a vital role in accumulation and dispersion of atmospheric pollutants (Xu et al.,

190     2011;Zheng et al., 2015b). For example, the relatively high levels of $PM_{2.5}$ (>100 μg m$^{-3}$) usually

191     occurred under the relatively stable meteorological conditions with the low south wind speed (<2

192     m s$^{-1}$) and the high RH (>60 %) which favored the accumulation of pollutants. Besides

193     meteorological conditions, the extremely high concentrations of the species in $PM_{2.5}$ might be

194     mainly ascribed to strong emissions of primary pollutants and rapid formation of secondary

195     aerosols during the wintertime in Beijing.

196     The average concentrations of the species in $PM_{2.5}$ and typical gaseous pollutants during

197     clean or slightly polluted (C&SP) episodes ($PM_{2.5}$<75 μg m$^{-3}$), during polluted or heavy polluted

198     (P&HP) episodes ($PM_{2.5}$≥75 μg m$^{-3}$) and during the whole sampling period are illustrated in Table

199     1. It is evident that the average concentrations of $NO_3^-$, $SO_4^{2-}$, $NH_4^+$, OC and EC during P&HP

200     episodes were about a factor of 5.0, 4.1, 6.1, 3.6 and 3.2 greater than those during C&SP episodes,

201     respectively, indicating that the formations of SIAs were more efficient compared to other species

202     in $PM_{2.5}$ during the serious pollution episodes. Given that the average concentrations of gaseous

203     precursors ($NO_2$ and $SO_2$) during P&HP episodes were approximately a factor of 2.0-2.2 greater

204    than those during C&SP episodes, the obviously higher elevation of $NO_3^-$ and $SO_4^{2-}$ implied that

205    the oxidations of $NO_2$ and $SO_2$ by the major atmospheric oxidizing agents (OH radicals, $O_3$ and

206    $H_2O_2$ etc.) might be greatly accelerated due to the relatively high concentrations of oxidants and

207    atmospheric RH during the serious pollution episodes (Figure 1). The average concentration of

208    $H_2O_2$ was found to be a factor of 1.7 greater during P&HP episodes than during C&SP episodes,

209    indicating that atmospheric $H_2O_2$ might contribute to the formation of SIAs especially sulfate

210    during the serious pollution episodes with high atmospheric RH, which will be discussed in Sect.

211    3.3.2. However, the obvious decrease in $O_3$ average concentration was observed during P&HP

212    episodes compared to C&SP episodes, which was mainly attributed to the relatively weak solar

213    radiation and the titration of NO during the serious pollution episodes (Ye et al., 2018). In addition,

214    the evidently higher average concentration of HONO during P&HP episodes than during C&SP

215    episodes might be also due to the relatively weak solar radiation as well as the heterogeneous

216    reaction of $NO_2$ on particle surfaces during the serious pollution episodes (Tong et al., 2016; Wang

217    et al., 2017).

218    **3.2. Three serious pollution cases during the sampling period**

219         Based on the transition from the clean to polluted periods, three haze cases were identified

220    during the sampling period (Figure 1 and Figure S2): from 13:00 on January 8th to 1:00 on January

221    11th (Case 1), from 14:00 on January 14th to 7:00 on January 17th (Case 2), and from 8:00 on

222    January 19th to 2:00 on January 22nd (Case 3). The serious pollution duration in the three cases

223    could last 1-3 days due to the differences of their formation mechanisms.

224         In Case 1, the variation trends of the concentrations of the species in $PM_{2.5}$, $NO_x$, $SO_2$,

225    HONO and $H_2O_2$ were almost identical and exhibited three pollution peaks at night (Figure 1),

226    which might be ascribed to the possibility that the decrease of nocturnal mixed boundary layer

227    accelerated the pollutant accumulation (Bei et al., 2017;Zhong et al., 2019). Considering the

228    relatively low RH (15-40 %) and wind speeds (<2 m s$^{-1}$) in Case 1 (Figure S2), primary emissions

229    around the sampling site were suspected to be a dominant source for the increase in the PM$_{2.5}$

230    concentrations. Further evidence is that the correlation between the concentrations of PM$_{2.5}$ and

231    CO is better in Case 1 (R$^2$=0.55) than in Case 2 and Case 3 (R$^2$=0.20~0.52) (Figure S3). Identical

232    to Case 1, three obvious pollution peaks were also observed in Case 2 (Figure 1). The variation

233    trends of the concentrations of the species in PM$_{2.5}$ and typical gaseous pollutants at the first peak

234    in Case 2 were found to be similar with those in Case 1, which were mainly attributed to their

235    similar formation mechanism. However, the evident decreases in NO$_x$ and SO$_2$ were observed

236    when the concentrations of the species in PM$_{2.5}$ were increasing and the atmospheric oxidation

237    pollutant (e.g. H$_2$O$_2$) concentration peaks were prior to others at the last two peaks in Case 2,

238    suggesting that secondary formation from gaseous precursors might be dominant for PM$_{2.5}$

239    pollution. The relatively high RH (50-80 %) and the low south wind speeds (<2 m s$^{-1}$) in Case 2

240    (Figure S2) provided further evidence for the above speculation. In contrast to Case 1 and Case 2,

241    the relatively high south wind speeds (>3 m s$^{-1}$) (Figure S2) with the concentrations of the species

242    in PM$_{2.5}$ and typical gaseous pollutants increasing slowly (Figure 1) at the beginning of Case 3

243    indicated that regional transportation might be responsible for the atmospheric species.

244    Subsequently, the concentrations of the species in PM$_{2.5}$ remained relatively high when the

245    atmospheric RH lasted more than 60 %, implying that secondary formation from gaseous

246    precursors dominated PM$_{2.5}$ pollution during the late period of Case 3.

247        The average mass proportions of the species in PM$_{2.5}$ in the three cases are illustrated in

248    Figure S4, the proportions of the primary species such as EC (10-13 %), Cl⁻ (6-7 %) and Na⁺ (4 %)

249    in the three cases were almost identical, indicating that primary particle emissions were relatively

250    stable during the sampling period. However, the proportions of SIA in Case 2 (42 %) and Case 3

251    (38 %) were conspicuously greater than that in Case 1 (28 %), further confirming that secondary

252    formation of inorganic ions (e.g. nitrate, sulfate) made a significant contribution to atmospheric

253    $PM_{2.5}$ in Case 2 and Case 3.

254    **3.3. Formation mechanism of nitrate and sulfate during serious pollution episodes**

255    As for nitrate and sulfate in the three cases, the highest mass proportion (18 %) of nitrate was

256    observed in Case 2, whereas the highest mass proportion (15 %) of sulfate was found in Case 3

257    (Figure S4). Although the concentrations of $SO_2$ were about a factor of 5 lower than the

258    concentrations of $NO_2$ in both Case 2 and Case 3 (Figure 1), the extremely high proportion of

259    sulfate in Case 3 might be ascribed to the long-lasting plateau of RH (Figure S2) because the

260    aqueous-phase reaction could accelerate the conversion of $SO_2$ to $SO_4^{2-}$. To further investigate the

261    pollution characteristics of nitrate and sulfate during the serious pollution episodes, the relations

262    between NOR (NOR = $NO_3^-$ / ($NO_3^-$+$NO_x$)) as well as SOR (SOR = $SO_4^{2-}$ / ($SO_4^{2-}$+$SO_2$)) and RH

263    are shown in Figure 2. There were obvious differences in the variations of NOR and SOR under

264    different atmospheric RH conditions. The variation trends of NOR and SOR almost stayed the

265    same when atmospheric RH was below 30 %, and then simultaneously increased with atmospheric

266    RH in the range of 30-60 %. The enhanced gas-phase reaction and the heterogeneous reaction

267    involving aerosol liquid water might make a remarkable contribution to the elevation of NOR and

268    SOR, respectively, which were further discussed in the following section. Subsequently, the

269    variation trend of NOR slowly decreased whereas the variation trend of SOR significantly

Atmospheric
Chemistry
and Physics
Discussions

270    increased when atmospheric RH was above 60 %. The reduction of NOR might be due to the

271    deliquescence of nitrate at atmospheric RH around 60 % (Kuang et al., 2016;Liu et al., 2016b;Xue

272    et al., 2014), while the elevation of SOR revealed the dominant contribution of the aqueous-phase

273    reaction to the formation of sulfate.

274    **3.3.1. Formation mechanism of nitrate**

275        Atmospheric nitrate is considered to be mainly from $NO_2$ oxidation by OH radical in the gas

276    phase, heterogeneous uptake of $NO_2$ on the surface of particles and heterogeneous hydrolysis of

277    $N_2O_5$ on wet aerosols or chloride-containing aerosols (He et al., 2014;He et al., 2018;Nie et al.,

278    2014;Ravishankara, 1997;Wang et al., 2018b). Since atmospheric $N_2O_5$ is usually produced by the

279    reaction of $NO_3$ radical with $NO_2$ as well as both $NO_3$ radical and $N_2O_5$ are easily photolytic

280    during the daytime, the heterogeneous hydrolysis of $N_2O_5$ is a nighttime pathway for the

281    formation of atmospheric nitrate (He et al., 2018;Wang et al., 2018b). As shown in Figure 3a, the

282    mean values of NOR during the nighttime remarkably elevated with atmospheric RH increasing,

283    the disproportionation of $NO_2$ and the heterogeneous hydrolysis of $N_2O_5$ involving aerosol liquid

284    water were suspected to dominate the nocturnal formation of nitrate under high RH conditions

285    during the sampling period (Ma et al., 2017;Wang et al., 2018b;Li et al., 2018). However, the

286    productions of HONO and nitrate should be equal through the disproportionation of $NO_2$ (Ma et

287    al., 2017), which could not explain the wide gaps between the average concentrations of HONO

288    (about 6.5 μg m$^{-3}$) and nitrate (about 20.1 μg m$^{-3}$) observed at the nighttime under high RH

289    conditions during the sampling period. Thus, the disproportionation of $NO_2$ made insignificant

290    contribution to the nocturnal formation of nitrate under high RH conditions. Considering that the

291    formation of atmospheric $NO_3$ radical is mainly via the oxidation of $NO_2$ by $O_3$, the heterogeneous

292    hydrolysis of $N_2O_5$ occurs only at high $O_3$ and $NO_2$ levels during the nighttime (He et al.,

293    2018;Wang et al., 2018b). Therefore, the correlation between $NO_2 \times O_3$ and NOR can represent

294    roughly the contribution of the heterogeneous hydrolysis of $N_2O_5$ to atmospheric nitrate at night.

295    As shown in Figure 3b, the more significant correlation between $NO_2 \times O_3$ and NOR under the

296    RH≥60 % condition ($R^2$=0.534) than under the RH<60 % condition ($R^2$<0.005) at the nighttime

297    (19:00-6:00) during the sampling period further confirmed that the heterogeneous hydrolysis of

298    $N_2O_5$ on wet aerosols made a great contribution to atmospheric nocturnal nitrate under high RH

299    conditions.

300    However, the obvious increase in the mean values of NOR during the daytime (especially for

301    10:00-17:00) under the 30 %<RH<60 % condition (Figure 3a) indicated that additional sources

302    rather than the heterogeneous hydrolysis of $N_2O_5$ were responsible for the formation of nitrate. To

303    explore the possible formation mechanisms of nitrate in this case, the daily variations of Dust (the

304    sum of $Ca^{2+}$ and $Mg^{2+}$) $\times NO_2$ and HONO (the main source of OH) $\times$ DR $\times NO_2$, which can

305    represent roughly the heterogeneous reaction of $NO_2$ on the surface of mineral aerosols and the

306    gas-phase reaction of $NO_2$ with OH, are shown in Figure 3c and Figure 3d, respectively. The mean

307    values of HONO $\times$ DR $\times NO_2$ during the daytime were found to be remarkably greater under the

308    30 %<RH<60 % condition than under the RH≤30 % condition, whereas the mean values of Dust $\times$

309    $NO_2$ almost stayed the same under the two different RH conditions. Considering the coincident

310    trend of NOR and HONO $\times$ DR $\times NO_2$ during the daytime (10:00-17:00) under the 30 %<RH<60 %

311    condition, the gas-phase reaction of $NO_2$ with OH played a key role in the diurnal formation of

312    nitrate at moderate RH levels with the haze pollution accumulating. It should be noted that the

313    mean values of HONO $\times$ DR $\times NO_2$ decreased dramatically from 14:00 to 17:00 (Figure 3d),

314    which was not responsible for the high mean values of NOR at that time (Figure 3a). However, the

315    slight increase in the mean values of Dust × $NO_2$ after 14:00 was observed under the

316    30 %<RH<60 % condition (Figure 3c) and hence the heterogeneous reaction of $NO_2$ on the

317    surface of mineral aerosols was suspected to contribute to the diurnal formation of nitrate at that

318    time under moderate RH condition.

319    **3.3.2. Formation mechanism of sulfate**

320    Atmospheric sulfate is principally from $SO_2$ oxidation pathway, including gas-phase

321    reactions with OH radical or stabilized Criegee intermediates, heterogeneous-phase reactions on

322    the surface of particles and aqueous-phase reactions with dissolved $O_3$, $NO_2$, $H_2O_2$ and organic

323    peroxides, as well as autoxidation catalyzed by TMI (Cheng et al., 2016;Li et al.,

324    2018;Ravishankara, 1997;Shao et al., 2019;Wang et al., 2016;Xue et al., 2016;Zhang et al., 2018).

325    As shown in Figure 4, similar to the daily variations of NOR, the remarkable elevation of the

326    mean values of SOR after 14:00 under the 30 %<RH<60 % condition compared to the RH≤30 %

327    condition might be also ascribed to the heterogeneous reaction of $SO_2$ on the surface of mineral

328    aerosols. The extremely high mean values of SOR during the whole day under the RH≥60 %

329    condition implied that aqueous oxidation of $SO_2$ dominated the formation of sulfate during the

330    severe pollution episodes, which was in line with previous studies (Zhang et al., 2018;Cheng et al.,

331    2016). A key factor that influenced the aqueous oxidation pathways for sulfate formation has been

332    considered to be the aerosol pH (Guo et al., 2017;Liu et al., 2017a), varying from 4.5 to 8.5 at

333    different atmospheric RH and sulfate levels during the sampling period (Figure 5a) on the basis of

334    the ISORROPIA-II model. Considering that the aqueous-phase chemistry of sulfate formation

335    usually occurs in severe haze events with relatively high atmospheric RH, the aerosol pH (4.5-5.3)

336    under the RH≥60 % condition, which was lower than those (5.4-7.0) in the studies of Wang et al.,

337    (2016) and Cheng et al., (2016) but was slightly higher than those (3.0-4.9) in the studies of Liu et

338    al., (2017a) and Guo et al., (2017), was adopted for evaluating sulfate production in this study. In

339    addition, in terms of oxidants, the obvious increase in the average concentration of $NO_2$ (Figure 5b)

340    and the evident decrease in the average concentration of $O_3$ (Figure 5d) were observed with the

341    deterioration of $PM_{2.5}$ pollution. Furthermore, the average concentration of $H_2O_2$ was also found

342    to be extremely high (0.25 ppb) under the HP condition (Figure 5c) and was above 1 order of

343    magnitude higher than that (0.01 ppb) assumed by Cheng et al., (2016), which probably resulted in

344    the underestimation of the contribution of $H_2O_2$ to sulfate formation in the study of Cheng et al.,

345    (2016).

346        To further explore the contribution of $H_2O_2$ to sulfate production rate under the HP condition,

347    the parameters measured in this study (Table 2) and the same approach that was adopted by Cheng

348    et al., (2016) were used to calculate sulfate production. As shown in Figure 6, the relationships

349    between different aqueous oxidation pathways and aerosol pH in this study were found to be very

350    similar with those of Cheng et al., (2016). However, the contribution of $H_2O_2$ to sulfate production

351    rate was about a factor of 17 faster in this study (about 1.16 μg m$^{-3}$ h$^{-1}$) than in the study (about

352    6.95×10$^{-2}$ μg m$^{-3}$ h$^{-1}$) of Cheng et al., (2016), implying that the contribution of $H_2O_2$ to sulfate

353    formation was largely neglected. Furthermore, considering the aerosol pH calculated under the HP

354    condition during the sampling period, the oxidation pathway of $NO_2$ might play an insignificant

355    role in sulfate production rate (8.96×10$^{-2}$-0.56 μg m$^{-3}$ h$^{-1}$) and its importance proposed by the

356    previous studies (1.74-10.85 μg m$^{-3}$ h$^{-1}$) was not necessarily expected.

357    **4. Conclusion**

358    Based on the comprehensive analysis of the pollution levels, the variation characteristics and

359    the formation mechanisms of the key species in $PM_{2.5}$ and the typical gaseous pollutants during

360    the winter haze pollution periods in Beijing, three serious haze pollution cases were obtained

361    during the sampling period and the SIAs formations especially nitrate and sulfate were found to

362    make an evident contribution to atmospheric $PM_{2.5}$ under the relatively high RH condition. The

363    significant correlation between $NO_2 \times O_3$ and NOR at night under the RH≥60 % condition

364    indicated that the heterogeneous hydrolysis of $N_2O_5$ on wet aerosols was responsible for the

365    nocturnal formation of nitrate under extremely high RH conditions. The more coincident trend of

366    NOR and $HONO \times DR \times NO_2$ than $Dust \times NO_2$ during the daytime under the 30 %<RH<60 %

367    condition suggested that the gas-phase reaction of $NO_2$ with OH played a key role in the diurnal

368    formation of nitrate under moderate RH conditions. The extremely high mean values of SOR

369    during the whole day under the RH≥60 % condition could be explained by the dominant

370    contribution of aqueous-phase reaction of $SO_2$ to atmospheric sulfate formation during the severe

371    pollution episodes. According to the parameters measured in this study and the same approach that

372    was adopted by Cheng et al., (2016), the oxidation pathway of $H_2O_2$ rather than $NO_2$ was found to

373    contribute greatly to atmospheric sulfate formation.

374    Our results revealed that the heavy pollution events in winter usually occurred with high

375    concentration levels of pollutants and oxidants as well as high liquid water contents of moderately

376    acidic aerosols in the NCP. Thus, emission controls of $NO_x$, $SO_2$ and VOCs especially under the

377    extremely high RH conditions are expected to reduce largely the pollution levels of nitrate and

378    sulfate in northern China and even in other pollution regions of China.

379

380    *Data availability.* Data are available from the corresponding author upon request

381    (yjmu@rcees.ac.cn)

382

383    *Author contributions.* YJM designed the experiments. PFL carried out the experiments and

384    prepared the manuscript. CY and CYX carried out the experiments. CLZ was involved in part of

385    the work. XS provided the meteorological data and trace gases in Beijing.

386

387    *Competing interests.* The authors declare that they have no conflict of interest.

388

395

Atmospheric
Chemistry
and Physics
Discussions
Open Access
EGU
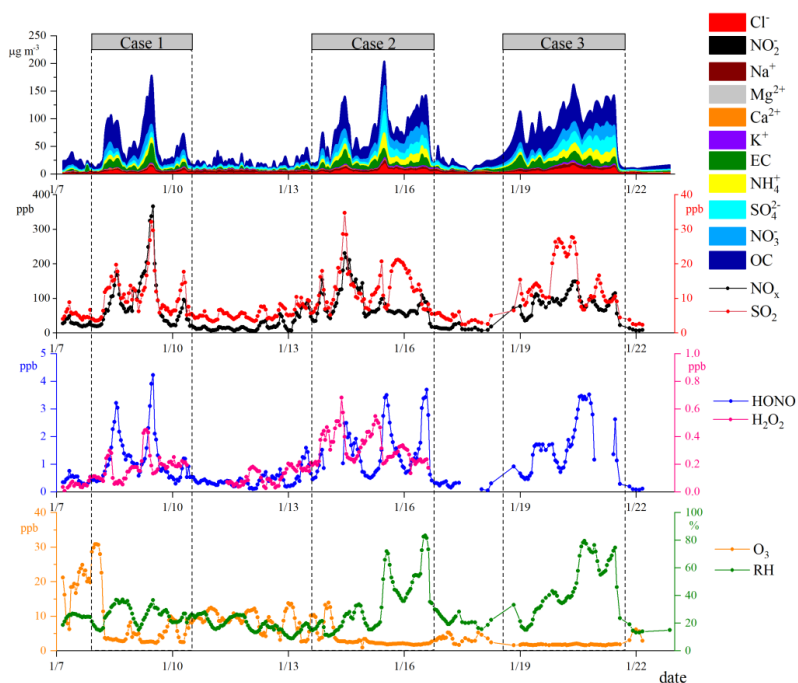
**Figure 1.** Time series of the species in PM$_{2.5}$ and typical gaseous pollutants (NO$_x$, SO$_2$, O$_3$, HONO and H$_2$O$_2$) as well as atmospheric RH during the sampling period.
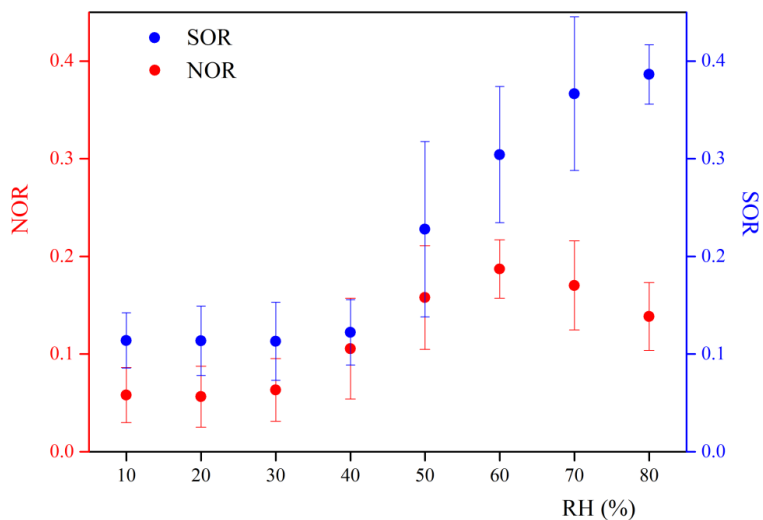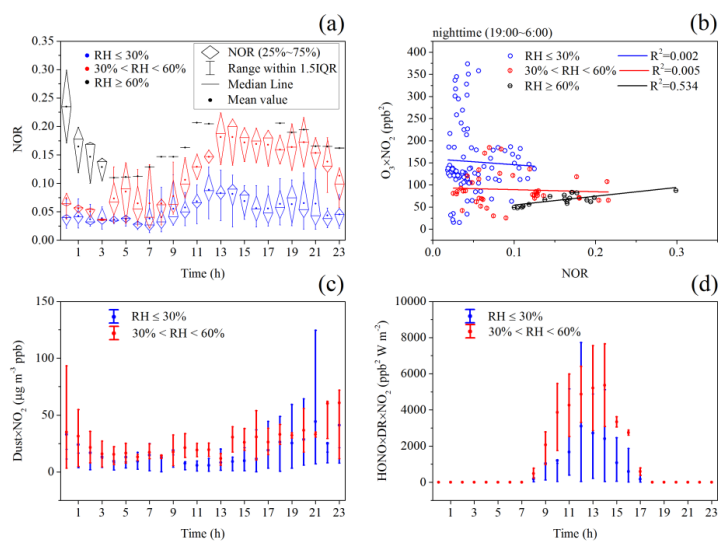


**Figure 2.** The relations between NOR as well as SOR and RH during the sampling period.

Atmospheric
Chemistry
and Physics
Discussions

Open Access
EGU

402



403

404 **Figure 3.** Daily variation of NOR (a), the correlation between NOR and $O_3 \times NO_2$ at the nighttime
405 (b), daily variations of Dust$\times NO_2$ and HONO$\times$DR$\times NO_2$ (c, d) under different atmospheric RH
406 conditions during the sampling period.
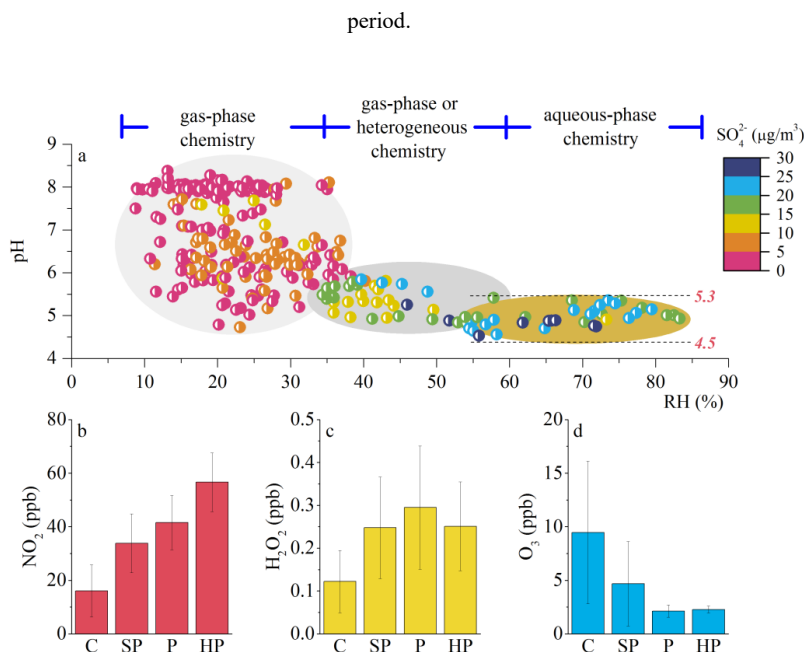
407
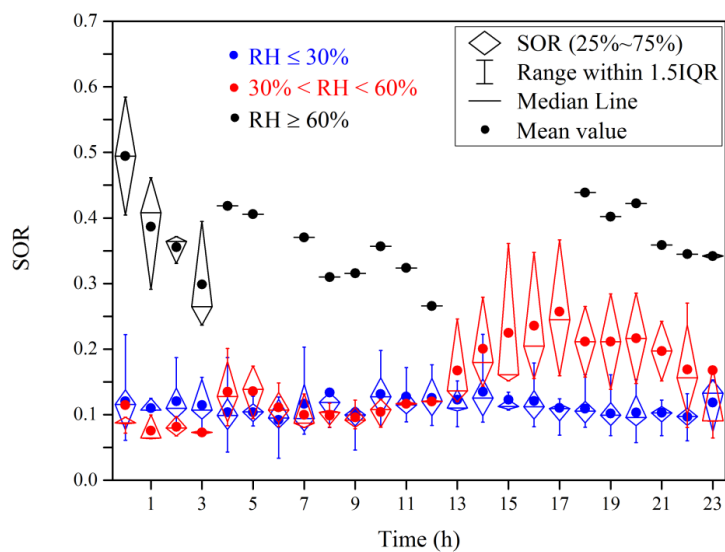


408

409 **Figure 4.** Daily variation of SOR under different atmospheric RH conditions during the sampling
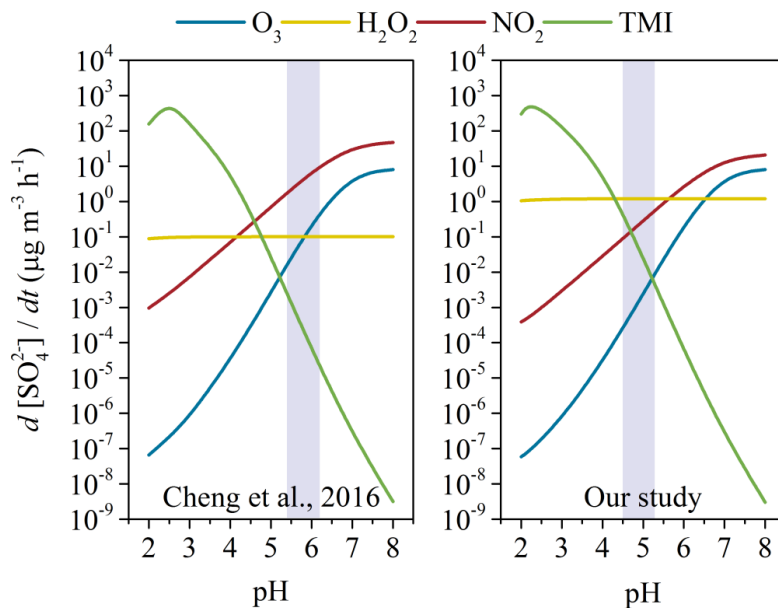
410                                                         period.

411



412

413     **Figure 5.** The correlations among aerosol pH, atmospheric RH and atmospheric $SO_4^{2-}$ (a), the

414     average concentrations of $NO_2$, $H_2O_2$ and $O_3$ (b, c, d) under different pollution conditions (clean

415     (C), $PM_{2.5}<35$ μg m$^{-3}$; slightly polluted (SP), 35 μg m$^{-3}<PM_{2.5}<75$ μg m$^{-3}$; polluted (P), 75 μg

416     m$^{-3}<PM_{2.5}<150$ μg m$^{-3}$; heavy polluted (HP), $PM_{2.5}>150$ μg m$^{-3}$) during the sampling period.

417

418

**Figure 6.** The comparison of aqueous-phase sulfate production by $SO_2$ oxidation under different aerosol pH conditions between in the study of Cheng et al., (2016) and in this study.

**Table 1.** The average concentrations of the species in $PM_{2.5}$ ($\mu g\ m^{-3}$) and typical gaseous pollutants (ppb) during C&SP episodes ($PM_{2.5}<75\ \mu g\ m^{-3}$), during P&HP episodes ($PM_{2.5}\geq75\ \mu g\ m^{-3}$) and during the whole sampling period.

| species | during C&SP episodes (n=210) | during P&HP episodes (n=108) | total (n=318) |
|---|---|---|---|
| $PM_{2.5}$ | $30.00 \pm 17.79$ | $113.35 \pm 28.10$ | $58.31 \pm 45.15$ |
| $Na^+$ | $2.88 \pm 1.11$ | $3.68 \pm 1.19$ | $3.15 \pm 1.21$ |
| $Mg^{2+}$ | $0.05 \pm 0.03$ | $0.08 \pm 0.06$ | $0.06 \pm 0.04$ |
| $Ca^{2+}$ | $0.52 \pm 0.33$ | $0.67 \pm 0.48$ | $0.58 \pm 0.40$ |
| $K^+$ | $0.81 \pm 0.42$ | $1.84 \pm 0.73$ | $1.16 \pm 0.73$ |
| $NH_4^+$ | $1.90 \pm 1.90$ | $11.52 \pm 4.93$ | $5.17 \pm 5.62$ |
| $SO_4^{2-}$ | $3.64 \pm 1.87$ | $14.96 \pm 7.80$ | $7.47 \pm 7.18$ |
| $NO_3^-$ | $3.44 \pm 3.57$ | $17.15 \pm 7.36$ | $8.10 \pm 8.32$ |
| $Cl^-$ | $1.89 \pm 1.20$ | $7.35 \pm 2.97$ | $3.73 \pm 3.26$ |
| $NO_2^-$ | $0.06 \pm 0.08$ | $0.06 \pm 0.05$ | $0.06 \pm 0.07$ |
| OC | $12.10 \pm 9.25$ | $43.34 \pm 13.88$ | $22.73 \pm 18.48$ |
| EC | $3.98 \pm 3.42$ | $12.69 \pm 6.43$ | $7.58 \pm 6.51$ |
| $NO_x$ | $39.38 \pm 35.25$ | $107.71 \pm 58.44$ | $62.59 \pm 54.98$ |
| $NO_2$ | $21.46 \pm 13.04$ | $42.81 \pm 10.96$ | $28.71 \pm 15.98$ |
| $SO_2$ | $6.99 \pm 3.64$ | $15.70 \pm 6.55$ | $9.95 \pm 6.35$ |
| $O_3$ | $8.01 \pm 6.35$ | $2.13 \pm 0.56$ | $6.01 \pm 5.87$ |
| HONO | $0.60 \pm 0.43$ | $1.90 \pm 0.97$ | $1.01 \pm 0.87$ |
| $H_2O_2$ | $0.17 \pm 0.11$ | $0.29 \pm 0.14$ | $0.20 \pm 0.13$ |

**Table 2.** The comparisons for parameters of sulfate production rate calculations between in the study of Cheng et al., (2016) and in this work during the most polluted haze periods

| Parameters | This study | Cheng et al., (2016) |
|---|---|---|
| $NO_2$ | 57 ppb | 66 ppb |
| $H_2O_2$ | 0.25 ppb | 0.01 ppb |
| $O_3$ | 2 ppb | 1 ppb |
| $SO_2$ | 35 ppb | 40 ppb |
| Fe(III)[a] | 18 ng $m^{-3}$ | 18 ng $m^{-3}$ |
| Mn(II)[a] | 42 ng $m^{-3}$ | 42 ng $m^{-3}$ |
| ALWC | 146 $\mu g\ m^{-3}$ | 300 $\mu g\ m^{-3}$ |
| Aerosol droplet radius (R)[a] | 0.15 $\mu m$ | 0.15 $\mu m$ |
| Temperature | 270 K | 271 K |
| pH | 4.5-5.3 | 5.4-6.2 |

[a]: both the concentrations of Fe(III) and Mn(II) and aerosol droplet radius were not measured in this study and were derived from Cheng et al., (2016).

**References**

432    Bei, N., Wu, J., Elser, M., Feng, T., Cao, J., El-Haddad, I., Li, X., Huang, R., Li, Z., Long, X., Xing, L.,
433    Zhao, S., Tie, X., Prévôt, A. S. H., and Li, G.: Impacts of meteorological uncertainties on the haze
434    formation in Beijing–Tianjin–Hebei (BTH) during wintertime: a case study, Atmospheric Chemistry
435    and Physics, 17, 14579-14591, 10.5194/acp-17-14579-2017, 2017.
436    Bougiatioti, A., Nikolaou, P., Stavroulas, I., Kouvarakis, G., Weber, R., Nenes, A., Kanakidou, M., and
437    Mihalopoulos, N.: Particle water and pH in the eastern Mediterranean: source variability and
438    implications for nutrient availability, Atmospheric Chemistry and Physics, 16, 4579-4591,
439    10.5194/acp-16-4579-2016, 2016.
440    Chan, C. K., and Yao, X.: Air pollution in mega cities in China, Atmospheric Environment, 42, 1-42,
441    10.1016/j.atmosenv.2007.09.003, 2008.
442    Chen, L. H., Sun, Y. Y., Wu, X. C., Zhang, Y. X., Zheng, C. H., Gao, X., and Cen, K.: Unit-based
443    emission inventory and uncertainty assessment of coal-fired power plants, Atmospheric Environment,
444    99, 527-535, 10.1016/j.atmosenv.2014.10.023, 2014.
445    Cheng, Y., Zheng, G., Wei, C., Mu, Q., Zheng, B., Wang, Z., Gao, M., Zhang, Q., He, K., Carmichael,
446    G., Pöschl, U., and Su, H.: Reactive nitrogen chemistry in aerosol water as a source of sulfate during
447    haze events in China, Science Advances, 2, 1-11, 10.1126/sciadv.1601530, 2016.
448    Clifton, C. L., Altstein, N., and Huie, R. E.: Rate-constant for the reaction of $NO_2$ with sulfur(IV) over
449    the pH range 5.3-13, Environ. Sci. Technol., 22, 586-589, 10.1021/es00170a018, 1988.
450    Dai, Q., Bi, X., Song, W., Li, T., Liu, B., Ding, J., Xu, J., Song, C., Yang, N., Schulze, B. C., Zhang, Y.,
451    Feng, Y., and Hopke, P. K.: Residential coal combustion as a source of primary sulfate in Xi'an, China,
452    Atmospheric Environment, 196, 66-76, 10.1016/j.atmosenv.2018.10.002, 2019.
453    Ding, J., Zhao, P., Su, J., Dong, Q., Du, X., and Zhang, Y.: Aerosol pH and its driving factors in Beijing,
454    Atmospheric Chemistry and Physics, 19, 7939-7954, 10.5194/acp-19-7939-2019, 2019.
455    Du, Q., Zhang, C., Mu, Y., Cheng, Y., Zhang, Y., Liu, C., Song, M., Tian, D., Liu, P., Liu, J., Xue, C.,
456    and Ye, C.: An important missing source of atmospheric carbonyl sulfide: Domestic coal combustion,
457    Geophysical Research Letters, 43, 8720-8727, 10.1002/2016gl070075, 2016.
458    Fountoukis, C., and Nenes, A.: ISORROPIA II: a computationally efficient thermodynamic equilibrium
459    model for $K^+$-$Ca^{2+}$-$Mg^{2+}$-$NH_4^+$-$Na^+$-$SO_4^{2-}$-$NO_3^-$-$Cl^-$-$H_2O$ aerosols, Atmospheric Chemistry and Physics,
460    7, 4639-4659, 2007.
461    Ge, X., He, Y., Sun, Y., Xu, J., Wang, J., Shen, Y., and Chen, M.: Characteristics and Formation
462    Mechanisms of Fine Particulate Nitrate in Typical Urban Areas in China, Atmosphere, 8, 62,
463    10.3390/atmos8030062, 2017.
464    Graedel, T. E., and Weschler, C. J.: Chemistry within aqueous atmospheric aerosols and raindrops,
465    Reviews of Geophysics, 19, 505-539, 10.1029/RG019i004p00505, 1981.
466    Guo, H., Xu, L., Bougiatioti, A., Cerully, K. M., Capps, S. L., Hite, J. R., Carlton, A. G., Lee, S. H.,
467    Bergin, M. H., Ng, N. L., Nenes, A., and Weber, R. J.: Fine-particle water and pH in the southeastern
468    United States, Atmospheric Chemistry and Physics, 15, 5211-5228, 10.5194/acp-15-5211-2015, 2015.
469    Guo, H., Weber, R. J., and Nenes, A.: High levels of ammonia do not raise fine particle pH sufficiently
470    to yield nitrogen oxide-dominated sulfate production, Scientific reports, 7, 12109,
471    10.1038/s41598-017-11704-0, 2017.
472    Guo, S., Hu, M., Zamora, M. L., Peng, J., Shang, D., Zheng, J., Du, Z., Wu, Z., Shao, M., Zeng, L.,
473    Molina, M. J., and Zhang, R.: Elucidating severe urban haze formation in China, Proceedings of the
474    National Academy of Sciences of the United States of America, 111, 17373-17378,
475    10.1073/pnas.1419604111, 2014.

476   He, H., Wang, Y., Ma, Q., Ma, J., Chu, B., Ji, D., Tang, G., Liu, C., Zhang, H., and Hao, J.: Mineral
477   dust and $NO_x$ promote the conversion of $SO_2$ to sulfate in heavy pollution days, Scientific reports, 4,
478   1-5, 10.1038/srep04172, 2014.

479   He, P., Xie, Z., Chi, X., Yu, X., Fan, S., Kang, H., Liu, C., and Zhan, H.: Atmospheric $\Delta17O(NO_3^-)$
480   reveals nocturnal chemistry dominates nitrate production in Beijing haze, Atmospheric Chemistry and
481   Physics, 18, 14465-14476, 10.5194/acp-18-14465-2018, 2018.

482   Hennigan, C. J., Izumi, J., Sullivan, A. P., Weber, R. J., and Nenes, A.: A critical evaluation of proxy
483   methods used to estimate the acidity of atmospheric particles, Atmospheric Chemistry and Physics, 15,
484   2775-2790, 10.5194/acp-15-2775-2015, 2015.

485   Huang, R. J., Zhang, Y., Bozzetti, C., Ho, K. F., Cao, J. J., Han, Y., Daellenbach, K. R., Slowik, J. G.,
486   Platt, S. M., Canonaco, F., Zotter, P., Wolf, R., Pieber, S. M., Bruns, E. A., Crippa, M., Ciarelli, G.,
487   Piazzalunga, A., Schwikowski, M., Abbaszade, G., Schnelle-Kreis, J., Zimmermann, R., An, Z., Szidat,
488   S., Baltensperger, U., El Haddad, I., and Prevot, A. S.: High secondary aerosol contribution to
489   particulate pollution during haze events in China, Nature, 514, 218-222, 10.1038/nature13774, 2014.

490   Ibusuki, T., and Takeuchi, K.: Sulfur-dioxide oxidation by oxygen catalyzed by mixtures of
491   manganese(II) and iron(III) in aqueous-solutions at environmental reaction conditions, Atmospheric
492   Environment, 21, 1555-1560, 10.1016/0004-6981(87)90317-9, 1987.

493   Kuang, Y., Zhao, C. S., Ma, N., Liu, H. J., Bian, Y. X., Tao, J. C., and Hu, M.: Deliquescent phenomena
494   of ambient aerosols on the North China Plain, Geophysical Research Letters, 43, 8744-8750,
495   10.1002/2016gl070273, 2016.

496   Li, G., Bei, N., Cao, J., Huang, R., Wu, J., Feng, T., Wang, Y., Liu, S., Zhang, Q., Tie, X., and Molina,
497   L. T.: A possible pathway for rapid growth of sulfate during haze days in China, Atmospheric
498   Chemistry and Physics, 17, 3301-3316, 10.5194/acp-17-3301-2017, 2017.

499   Li, J., Liao, H., Hu, J., and Li, N.: Severe particulate pollution days in China during 2013-2018 and the
500   associated typical weather patterns in Beijing-Tianjin-Hebei and the Yangtze River Delta regions,
501   Environ Pollut, 248, 74-81, 10.1016/j.envpol.2019.01.124, 2019.

502   Li, L., Hoffmann, M. R., and Colussi, A. J.: Role of nitrogen dioxide in the production of sulfate during
503   Chinese haze-aerosol episodes, Environ Sci Technol, 52, 2686-2693, 10.1021/acs.est.7b05222, 2018.

504   Li, Q., Li, X., Jiang, J., Duan, L., Ge, S., Zhang, Q., Deng, J., Wang, S., and Hao, J.: Semi-coke
505   briquettes: towards reducing emissions of primary $PM_{2.5}$, particulate carbon, and carbon monoxide
506   from household coal combustion in China, Scientific reports, 6, 1-10, 10.1038/srep19306, 2016.

507   Liu, M., Song, Y., Zhou, T., Xu, Z., Yan, C., Zheng, M., Wu, Z., Hu, M., Wu, Y., and Zhu, T.: Fine
508   particle pH during severe haze episodes in northern China, Geophysical Research Letters, 44, 1-9,
509   10.1002/2017GL073210, 2017a.

510   Liu, P., Zhang, C., Mu, Y., Liu, C., Xue, C., Ye, C., Liu, J., Zhang, Y., and Zhang, H.: The possible
511   contribution of the periodic emissions from farmers' activities in the North China Plain to atmospheric
512   water-soluble ions in Beijing, Atmospheric Chemistry and Physics, 16, 10097-10109,
513   10.5194/acp-16-10097-2016, 2016a.

514   Liu, P., Zhang, C., Xue, C., Mu, Y., Liu, J., Zhang, Y., Tian, D., Ye, C., Zhang, H., and Guan, J.: The
515   contribution of residential coal combustion to atmospheric $PM_{2.5}$ in northern China during winter,
516   Atmospheric Chemistry and Physics, 17, 11503-11520, 10.5194/acp-17-11503-2017, 2017b.

517   Liu, Q., Jing, B., Peng, C., Tong, S., Wang, W., and Ge, M.: Hygroscopicity of internally mixed
518   multi-component aerosol particles of atmospheric relevance, Atmospheric Environment, 125, 69-77,
519   10.1016/j.atmosenv.2015.11.003, 2016b.

520   Ma, Q., Wang, T., Liu, C., He, H., Wang, Z., Wang, W., and Liang, Y.: SO$_2$ Initiates the efficient
521   conversion of NO$_2$ to HONO on MgO Surface, Environ Sci Technol, 51, 3767-3775,
522   10.1021/acs.est.6b05724, 2017.
523   Meng, Z. Y., Lin, W. L., Jiang, X. M., Yan, P., Wang, Y., Zhang, Y. M., Jia, X. F., and Yu, X. L.:
524   Characteristics of atmospheric ammonia over Beijing, China, Atmospheric Chemistry and Physics, 11,
525   6139-6151, 10.5194/acp-11-6139-2011, 2011.
526   Murphy, J. G., Gregoire, P. K., Tevlin, A. G., Wentworth, G. R., Ellis, R. A., Markovic, M. Z., and
527   VandenBoer, T. C.: Observational constraints on particle acidity using measurements and modelling of
528   particles and gases, Faraday Discussions, 200, 379-395, 10.1039/c7fd00086c, 2017.
529   Nie, W., Ding, A., Wang, T., Kerminen, V. M., George, C., Xue, L., Wang, W., Zhang, Q., Petaja, T., Qi,
530   X., Gao, X., Wang, X., Yang, X., Fu, C., and Kulmala, M.: Polluted dust promotes new particle
531   formation and growth, Scientific reports, 4, 1-6, 10.1038/srep06634, 2014.
532   Pathak, R. K., Louie, P. K. K., and Chan, C. K.: Characteristics of aerosol acidity in Hong kong,
533   Atmospheric Environment, 38, 2965-2974, 10.1016/j.atmosenv.2004.02.044, 2004.
534   Quan, J., Tie, X., Zhang, Q., Liu, Q., Li, X., Gao, Y., and Zhao, D.: Characteristics of heavy aerosol
535   pollution during the 2012–2013 winter in Beijing, China, Atmospheric Environment, 88, 83-89,
536   10.1016/j.atmosenv.2014.01.058, 2014.
537   Ravishankara, A.: Heterogeneous and multiphase chemistry in the troposphere, Science, 276,
538   1058-1065, 1997.
539   Seinfeld, J. H., and Pandis, S. N.: Atmospheric Chemistry and Physics, from Air Pollution to Climate
540   Change, Wiley, 429-443 pp., 2006.
541   Shao, J., Chen, Q., Wang, Y., Lu, X., He, P., Sun, Y., Shah, V., Martin, R. V., Philip, S., Song, S., Zhao,
542   Y., Xie, Z., Zhang, L., and Alexander, B.: Heterogeneous sulfate aerosol formation mechanisms during
543   wintertime Chinese haze events: air quality model assessment using observations of sulfate oxygen
544   isotopes in Beijing, Atmospheric Chemistry and Physics, 19, 6107-6123, 10.5194/acp-19-6107-2019,
545   2019.
546   Shi, G., Xu, J., Peng, X., Xiao, Z., Chen, K., Tian, Y., Guan, X., Feng, Y., Yu, H., Nenes, A., and
547   Russell, A. G.: pH of aerosols in a polluted atmosphere: source contributions to highly acidic aerosol,
548   Environ Sci Technol, 51, 4289-4296, 10.1021/acs.est.6b05736, 2017.
549   Tham, Y. J., Wang, Z., Li, Q., Wang, W., Wang, X., Lu, K., Ma, N., Yan, C., Kecorius, S., Wiedensohler,
550   A., Zhang, Y., and Wang, T.: Heterogeneous N$_2$O$_5$ uptake coefficient and production yield of ClNO$_2$ in
551   polluted northern China: roles of aerosol water content and chemical composition, Atmospheric
552   Chemistry and Physics, 18, 13155-13171, 10.5194/acp-18-13155-2018, 2018.
553   Tong, S. R., Hou, S. Q., Zhang, Y., Chu, B. W., Liu, Y. C., He, H., Zhao, P. S., and Ge, M. F.: Exploring
554   the nitrous acid (HONO) formation mechanism in winter Beijing: direct emissions and heterogeneous
555   production in urban and suburban areas, Faraday Discussions, 189, 213-230, 10.1039/c5fd00163c,
556   2016.
557   Wang, G., Zhang, R., Gomez, M. E., Yang, L., Levy Zamora, M., Hu, M., Lin, Y., Peng, J., Guo, S.,
558   Meng, J., Li, J., Cheng, C., Hu, T., Ren, Y., Wang, Y., Gao, J., Cao, J., An, Z., Zhou, W., Li, G., Wang,
559   J., Tian, P., Marrero-Ortiz, W., Secrest, J., Du, Z., Zheng, J., Shang, D., Zeng, L., Shao, M., Wang, W.,
560   Huang, Y., Wang, Y., Zhu, Y., Li, Y., Hu, J., Pan, B., Cai, L., Cheng, Y., Ji, Y., Zhang, F., Rosenfeld, D.,
561   Liss, P. S., Duce, R. A., Kolb, C. E., and Molina, M. J.: Persistent sulfate formation from London Fog
562   to Chinese haze, Proceedings of the National Academy of Sciences of the United States of America,
563   113, 13630-13635, 2016.

564    Wang, G., Zhang, F., Peng, J., Duan, L., Ji, Y., Marrero-Ortiz, W., Wang, J., Li, J., Wu, C., Cao, C.,
565    Wang, Y., Zheng, J., Secrest, J., Li, Y., Wang, Y., Li, H., Li, N., and Zhang, R.: Particle acidity and
566    sulfate production during severe haze events in China cannot be reliably inferred by assuming a
567    mixture of inorganic salts, Atmospheric Chemistry and Physics, 18, 10123-10132,
568    10.5194/acp-18-10123-2018, 2018a.
569    Wang, H., Lu, K., Chen, X., Zhu, Q., Wu, Z., Wu, Y., and Sun, K.: Fast particulate nitrate formation via
570    $N_2O_5$ uptake aloft in winter in Beijing, Atmospheric Chemistry and Physics, 18, 10483-10495,
571    10.5194/acp-18-10483-2018, 2018b.
572    Wang, H., Lu, K., Guo, S., Wu, Z., Shang, D., Tan, Z., Wang, Y., Le Breton, M., Lou, S., Tang, M., Wu,
573    Y., Zhu, W., Zheng, J., Zeng, L., Hallquist, M., Hu, M., and Zhang, Y.: Efficient $N_2O_5$ uptake and $NO_3$
574    oxidation in the outflow of urban Beijing, Atmospheric Chemistry and Physics, 18, 9705-9721,
575    10.5194/acp-18-9705-2018, 2018c.
576    Wang, J., Zhang, X., Guo, J., Wang, Z., and Zhang, M.: Observation of nitrous acid (HONO) in Beijing,
577    China: Seasonal variation, nocturnal formation and daytime budget, The Science of the total
578    environment, 587-588, 350-359, 10.1016/j.scitotenv.2017.02.159, 2017.
579    Wang, Y., Yao, L., Wang, L., Liu, Z., Ji, D., Tang, G., Zhang, J., Sun, Y., Hu, B., and Xin, J.:
580    Mechanism for the formation of the January 2013 heavy haze pollution episode over central and
581    eastern China, Science China Earth Sciences, 57, 14-25, 10.1007/s11430-013-4773-4, 2013.
582    Weber, R. J., Guo, H., Russell, A. G., and Nenes, A.: High aerosol acidity despite declining
583    atmospheric sulfate concentrations over the past 15 years, Nature Geoscience, 9, 282-285,
584    10.1038/ngeo2665, 2016.
585    Wu, J., Bei, N., Hu, B., Liu, S., Zhou, M., Wang, Q., Li, X., Liu, L., Feng, T., Liu, Z., Wang, Y., Cao, J.,
586    Tie, X., Wang, J., Molina, L. T., and Li, G.: Is water vapor a key player of the wintertime haze in North
587    China Plain?, Atmospheric Chemistry and Physics, 19, 8721-8739, 10.5194/acp-19-8721-2019, 2019.
588    Xu, L., Duan, F., He, K., Ma, Y., Zhu, L., Zheng, Y., Huang, T., Kimoto, T., Ma, T., Li, H., Ye, S., Yang,
589    S., Sun, Z., and Xu, B.: Characteristics of the secondary water-soluble ions in a typical autumn haze in
590    Beijing, Environ Pollut, 227, 296-305, 10.1016/j.envpol.2017.04.076, 2017.
591    Xu, W. Y., Zhao, C. S., Ran, L., Deng, Z. Z., Liu, P. F., Ma, N., Lin, W. L., Xu, X. B., Yan, P., He, X.,
592    Yu, J., Liang, W. D., and Chen, L. L.: Characteristics of pollutants and their correlation to
593    meteorological conditions at a suburban site in the North China Plain, Atmospheric Chemistry and
594    Physics, 11, 4353-4369, 10.5194/acp-11-4353-2011, 2011.
595    Xue, C., Ye, C., Ma, Z., Liu, P., Zhang, Y., Zhang, C., Tang, K., Zhang, W., Zhao, X., Wang, Y., Song,
596    M., Liu, J., Duan, J., Qin, M., Tong, S., Ge, M., and Mu, Y.: Development of stripping coil-ion
597    chromatograph method and intercomparison with CEAS and LOPAP to measure atmospheric HONO,
598    The Science of the total environment, 646, 187-195, 10.1016/j.scitotenv.2018.07.244, 2019a.
599    Xue, C., Ye, C., Zhang, Y., Ma, Z., Liu, P., Zhang, C., Zhao, X., Liu, J., and Mu, Y.: Development and
600    application of a twin open-top chambers method to measure soil HONO emission in the North China
601    Plain, Sci. Total Environ., 659, 621-631, 10.1016/j.scitotenv.2018.12.245, 2019b.
602    Xue, J., Griffith, S. M., Yu, X., Lau, A. K. H., and Yu, J. Z.: Effect of nitrate and sulfate relative
603    abundance in $PM_{2.5}$ on liquid water content explored through half-hourly observations of inorganic
604    soluble aerosols at a polluted receptor site, Atmospheric Environment, 99, 24-31,
605    10.1016/j.atmosenv.2014.09.049, 2014.
606    Xue, J., Yuan, Z., Griffith, S. M., Yu, X., Lau, A. K., and Yu, J. Z.: Sulfate Formation Enhanced by a
607    Cocktail of High $NO_x$, $SO_2$, Particulate Matter, and Droplet pH during Haze-Fog Events in Megacities

608    in China: An Observation-Based Modeling Investigation, Environ Sci Technol, 50, 7325-7334,

609    10.1021/acs.est.6b00768, 2016.

610    Yang, T., Sun, Y., Zhang, W., Wang, Z., Liu, X., Fu, P., and Wang, X.: Evolutionary processes and

611    sources of high-nitrate haze episodes over Beijing, Spring, J Environ Sci (China), 54, 142-151,

612    10.1016/j.jes.2016.04.024, 2017.

613    Yang, Y. R., Liu, X. G., Qu, Y., An, J. L., Jiang, R., Zhang, Y. H., Sun, Y. L., Wu, Z. J., Zhang, F., Xu,

614    W. Q., and Ma, Q. X.: Characteristics and formation mechanism of continuous hazes in China: a case

615    study during the autumn of 2014 in the North China Plain, Atmospheric Chemistry and Physics, 15,

616    8165-8178, 10.5194/acp-15-8165-2015, 2015.

617    Ye, C., Liu, P., Ma, Z., Xue, C., Zhang, C., Zhang, Y., Liu, J., Liu, C., Sun, X., and Mu, Y.: High $H_2O_2$

618    Concentrations Observed during Haze Periods during the Winter in Beijing: Importance of $H_2O_2$

619    Oxidation in Sulfate Formation, Environmental Science & Technology Letters, 5, 757-763,

620    10.1021/acs.estlett.8b00579, 2018.

621    Zhang, H., Chen, S., Zhong, J., Zhang, S., Zhang, Y., Zhang, X., Li, Z., and Zeng, X. C.: Formation of

622    aqueous-phase sulfate during the haze period in China: Kinetics and atmospheric implications,

623    Atmospheric Environment, 177, 93-99, 10.1016/j.atmosenv.2018.01.017, 2018.

624    Zhang, Q., He, K. B., and Huo, H.: Cleaning China's air, Nature, 484, 161-162, 2012.

625    Zhang, R., Wang, G., Guo, S., Zamora, M. L., Ying, Q., Lin, Y., Wang, W., Hu, M., and Wang, Y.:

626    Formation of urban fine particulate matter, Chem Rev, 115, 3803-3855, 10.1021/acs.chemrev.5b00067,

627    2015.

628    Zhao, M., Wang, S., Tan, J., Hua, Y., Wu, D., and Hao, J.: Variation of Urban Atmospheric Ammonia

629    Pollution and its Relation with PM2.5 Chemical Property in Winter of Beijing, China, Aerosol and Air

630    Quality Research, 16, 1390-1402, 10.4209/aaqr.2015.12.0699, 2016.

631    Zheng, B., Zhang, Q., Zhang, Y., He, K. B., Wang, K., Zheng, G. J., Duan, F. K., Ma, Y. L., and Kimoto,

632    T.: Heterogeneous chemistry: a mechanism missing in current models to explain secondary inorganic

633    aerosol formation during the January 2013 haze episode in North China, Atmospheric Chemistry and

634    Physics, 15, 2031-2049, 10.5194/acp-15-2031-2015, 2015a.

635    Zheng, G. J., Duan, F. K., Su, H., Ma, Y. L., Cheng, Y., Zheng, B., Zhang, Q., Huang, T., Kimoto, T.,

636    Chang, D., Pöschl, U., Cheng, Y. F., and He, K. B.: Exploring the severe winter haze in Beijing: the

637    impact of synoptic weather, regional transport and heterogeneous reactions, Atmospheric Chemistry

638    and Physics, 15, 2969-2983, 10.5194/acp-15-2969-2015, 2015b.

639    Zhong, J., Zhang, X., Wang, Y., Wang, J., Shen, X., Zhang, H., Wang, T., Xie, Z., Liu, C., Zhang, H.,

640    Zhao, T., Sun, J., Fan, S., Gao, Z., Li, Y., and Wang, L.: The two-way feedback mechanism between

641    unfavorable meteorological conditions and cumulative aerosol pollution in various haze regions of

642    China, Atmospheric Chemistry and Physics, 19, 3287-3306, 10.5194/acp-19-3287-2019, 2019.

643